Contents lists available at ScienceDirect

Inorganica Chimica Acta

journal homepage: www.elsevier.com

Research paper

Oligopeptide models of the metal binding loop of the bacterial copper efflux regulator protein CueR as potential Cu(I) chelators

Edit Mesterházy[a, b], Bastien Boff[b], Colette Lebrun[b], Pascale Delangle[b, *], Attila Jancsó[a, *]

[a] Department of Inorganic and Analytical Chemistry, University of Szeged, Dóm tér 7, Szeged H-6720, Hungary
[b] INAC/SyMMES UMR 5819 CEA, CNRS, Université Grenoble Alpes, 17 rue des Martyrs, 38 054 Grenoble, France

ARTICLE INFO

Article history:
Received 20 April 2017
Received in revised form 20 June 2017
Accepted 27 June 2017
Available online xxx

Keywords:
Copper(I)
Competition
Peptide complexes
Thiolate coordination
Chelators

ABSTRACT

Copper(I) binding features of oligopeptides, mimicking the metal binding loops (MBL) of the bacterial copper efflux regulator protein CueR, were investigated with an aim of exploring potential candidates for Cu(I)-sequestration. Two of the studied ligands comprise the MBL of *E. coli* CueR (Ac-ACPGDDSADCPI-NH_2; **EC**) and *V. cholerae* CueR (Ac-SCPGDQGSDCPI-NH_2; **VC**) while the third peptide is a His-containing variant of **VC** (Ac-SCHGDQGSDCSI-NH_2; **HS**). UV-titrations of the ligands by Cu(I) at pH = 7.4 and monitoring the characteristic S_{Cys}^- → Cu(I) charge transfer bands, together with CD-experiments, indicated the exclusive formation of monomeric Cu(I)-complexes (CuL) up to a 1:1 Cu(I):L ratio and the presence of oligometallic/cluster type complexes at Cu(I)-excess. Such a change in speciation and the domination of the latter species was also supported by comparing the ESI-MS spectra obtained at 0.9:1 and 2:1 Cu(I):peptide ratios. pH-dependence of the UV spectra of the Cu(I):peptide 1:1 complexes reflected the formation of the two thiolate-Cu(I) bonds well below neutral pH, as two successive deprotonation processes could be fitted by apparent pK_a values falling in the pH range of 1.8–3.0 and 4.3–5.5. Cu(I)-binding affinity of the ligands was determined by competition experiments applying the bicinchoninate ion for the displacement of the Cu(I)-ligated peptides. The obtained conditional stability constants ($\log \beta_{11}^{pH7.4}$ = 15.3, 15.8 and 16.3 for Cu(**EC**), Cu(**VC**) and Cu(**HS**), respectively) indicate a strong affinity of Cu(I) to each ligand and suggest a slight destabilizing effect of charge repulsion between sidechain groups in **EC** while a possible Cu(I)-coordination of the histidine residue in **HS**.

1. Introduction

Copper is an essential element for life but in excess becomes toxic, therefore several proteins, with a wide range of metal binding motifs, participate in copper homeostasis [1]. Copper is found both in Cu(I) and Cu(II) oxidation states in living organisms. Cu(I) has a soft Lewis-acid character [2], and thus it is usually coordinated by 2, 3 or 4 sulphur donors in linear, trigonal planar or tetrahedral geometry [3]. The borderline Lewis-acid Cu(II) is generally coordinated by 4–6 nitrogen and oxygen donors in a square planar, (distorted) pentacoordinate or (distorted) octahedral geometries [3,4]. In copper binding proteins these donor atoms are provided by the thiolate moieties of cysteines, the thioether groups of methionines, the carboxylate groups of glutamates and aspartates, the imidazole rings of histidines, and besides, the N- and O-atoms of the polypeptide backbone can also play a role in the coordination of Cu(II).

The metal binding motifs of the various proteins participating in the sensing, transport or storage of copper in cellular compartments with a reducing environment perfectly accommodate this metal in its Cu(I) state. Metallothioneins, encompassing cysteine rich sequence patterns, e.g. CXC or CXXC, are known to participate in the detoxification of harmful metal overload [5]. These low molecular weight proteins are able to bind different number of Cu(I) ions in clusters [6,7]. A number of transport proteins utilize a variation of methionine and cysteine residues for the binding of Cu(I). Representative examples are the plasma membrane transporter Ctr1 with an 11-repeat consensus MxxM motif [8] or Cu-transporter P-type ATPases possessing a MxCxxC metal binding domain [9]. There are several other fascinating Cu(I)-binding sequences, such as the CxCxxxxCxC found in the CopY repressor protein of the *cop* operon [10], the methionine-rich LVMTAMPGMEHSPMGV Cu(I)-binding sequence of the periplasmic copper trafficking CopC [11], the unusual His36,Trp44,Met47,Met49 motif of the copper trafficking CusF [12,13] or the short CCxC fragment, which – together with three additional separated Cys residues – forms Cu(I)-clusters in the Cox17 chaperon [14].

The Cu(I)-responsive Cu Efflux Regulator CueR protein [15,16], a representative member of the large MerR family [17], regulates the synthesis of the copper transporter CopA [18] and the multicopper

* Corresponding authors.
Email addresses: pascale.delangle@cea.fr (P. Delangle); jancso@chem.u-szeged.hu (A. Jancsó)

http://dx.doi.org/10.1016/j.ica.2017.06.062
0020-1693/

oxidase CueO [19,20] at the transcription level. Each monomer of the dimeric CueR protein binds a Cu(I) ion by two conserved cysteine residues located at the two ends of a short loop, restricting the metal ion into a linear coordination fashion [21]. CueR displays an outstanding sensitivity for Cu(I) as it is able to sense Cu(I) in a zeptomolar (10^{-21} M) concentration. Besides, the protein can effectively differentiate between mono and divalent metal ions by providing a transcriptional response for Cu(I), Ag(I) or Au(I), but remaining inactive in the presence of Zn(II) or Hg(II) [21].

It has been previously demonstrated by Delangle et al. that short linear or cyclic decapeptides, inspired by the Cys-rich metal ion binding domains of proteins participating in the homeostasis of soft metal ions could be efficiently used for Cu(I)-chelation. The studied ligands, a linear and a cyclic peptide mimicking the metal binding MxCxxC motif of the Atx1 chaperon and two cyclodecapeptides containing two cysteine residues, displayed high affinity for Cu(I) and a high selectivity with regard to the potential cellular competitor Zn(II) [22–24].

With an aim of constructing potential peptide-based Cu(I)-sequestering ligands benefitting from the large sensitivity and selectivity of CueR, three 12-mer peptides were designed (Scheme 1). Two of the ligands comprise the metal binding loop of CueR found in *E. coli* (Ac-A**C**PGDDSAD**C**PI-NH_2; **EC**) and *V. cholerae* (Ac-S**C**PGDQGSD**C**PI-NH_2; **VC**). The third studied peptide is a variant of the ligand **VC**, where the two proline residues were replaced by a histidine and a serine (Ac-S**C**HGDQGSD**C**SI-NH_2; **HS**) with a purpose of influencing the flexibility and thus the metal binding properties of the molecule. His and Ser residues are, indeed, found in these positions in some of the metalloregulatory members of the MerR family [21]. Previously, we have reported on the Zn(II), Cd(II), Hg(II) and Ag(I) coordination features of these ligands [25–27]. In this work we present a detailed characterization of the Cu(I)-binding properties of the three 12-mer peptides, with a special attention devoted to the stability of species formed under neutral conditions with regard of their potential use in Cu(I)-chelation in medical applications [28].

2. Experimental

2.1. Materials

The investigated peptides were synthesized by solid phase synthesis following the standard Fmoc strategy and purified by reversed phase semi preparative HPLC, as described earlier [25]. Metal ion solutions were made of tetrakis(acetonitrile)copper(I) hexafluorophosphate ($Cu(CH_3CN)_4PF_6$, Aldrich) dissolved in acetonitrile (Sigma) and mercury(II) chloride ($HgCl_2$, Aldrich) dissolved in water. 5,5′-dithiobis-(2-nitrobenzoic acid) (DTNB) used for determining the concentration of the peptides, bathocuproinedisulfonic acid disodium salt (BCS) and bicinchoninic acid disodium salt hydrate (BCA) applied for determining the concentration of the copper(I) stock solutions and the conditional stability constants of the Cu(I) complexes, respectively, were purchased from Sigma-Aldrich. For the calibration of the mass spectrometry instrument a Pierce™ LTQ ESI Positive Ion Calibration Solution, containing Caffeine, MRFA and Ultramark 1621 was obtained from Thermo Fischer Scientific. Potassium phosphate monobasic (Sigma) and ammonium acetate (Acros) salts were used for buffer preparations. All the chemicals and solvents were used without further purification.

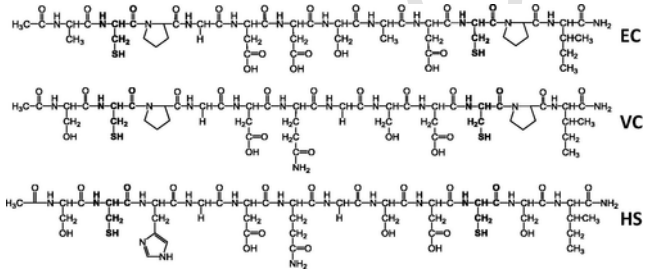

Scheme 1. Schematic structures of the studied peptides (*double column*).

2.2. Sample preparations

Since both the peptides and Cu(I) are sensitive to oxidation, all of the sample manipulations were performed in a glovebox under argon atmosphere. Fresh solutions were prepared before each experiment. The Cu(I) stock solution was prepared in acetonitrile to avoid Cu(I) disproportionation into Cu(0) and Cu(II). Indeed acetonitrile forms coordination complexes with Cu(I), which stabilizes the low oxidation state of copper in solution [29]. The peptides were dissolved in buffered media or in water containing 10 V/V% acetonitrile. The final concentration of the solutions was determined by Ellman's procedure [30,31]. The protocol uses DTNB; the $DTNB^{2-}$ anion reacts with free thiols resulting in the formation of the yellow colored TNB^- ion (2-nitro-5-thiobenzoate) per each thiol group (λ_{max} = 412 nm; ε = 14,150 M^{-1} cm^{-1}). The Cu(I) concentration of the stock solutions was determined by addition of excess BCS and measuring the absorbance of the $[Cu(BCS)_2]^{3-}$ complex (λ_{max} = 483 nm; ε = 13,300 M^{-1} cm^{-1}) [32].

2.3. UV spectroscopy

UV–Vis spectroscopic measurements were carried out on a Varian Cary50 spectrophotometer equipped with optical fibers connected to an external cell holder in the glove box. A quartz UV cell from Hellma Analytics with a 1.0 cm optical path length, equipped with a Teflon stopper, was used. For each titration 2.5 mL of a freshly prepared peptide solution ($c_{peptide} \sim 30$ μM, in phosphate buffer, pH = 7.4, c_{buffer} = 20 mM) were transferred to the cell. Aliquots of a Cu(I) stock solution ($c \sim 3$ mM), corresponding to 0.1 equivalent of Cu(I) per ligand, were added by a 10 μL capacity Hamilton syringe. For pH titrations 2.0 mL of the peptide stock solution ($c \sim 30$ μM) was transferred into the quartz UV cell and then 0.9 equivalent of Cu(I) was added. The desired pH values were adjusted with KOH solutions of appropriate concentrations (e.g. 0.1 M, 0.01 M). The pH of the solution was measured by a Metrohm 702 SM Titrino system equipped with a Mettler Toledo InLab® Microelectrode.

2.4. CD spectroscopy

Circular dichroism spectra were acquired on an Applied Photophysics Chirascan spectrometer. (1*S*)-(+)-10-camphorsulfonic acid served as calibration material for the instrument. 2.5 mL of freshly prepared peptide solution ($c_{peptide} \sim 80$ μM, in phosphate buffer, pH = 7.4, c_{buffer} = 20 mM) were transferred into a 1.0 cm optical path length sealable quartz cell (Hellma Analytics) with a silicone rubber seal. Aliquots of a Cu(I) stock solution ($c \sim 3$ mM), corresponding to 0.25 equivalents of Cu(I) per ligand, were added by a 10 μL capacity Hamilton syringe in the glove box. The spectra were recorded in the 190–400 nm wavelength range with 1 nm steps and a dwell time of 2 s per data points. The range of wavelength reported (typically 220–400 nm) corresponds to non-saturating CD signals, which was checked by looking at the HT voltage. Data were acquired and treated

by Pro-Data and Pro-Data Viewer programs (Applied Photophysics). From each sample 3 parallel spectra were recorded and the average of these spectra was smoothed by the Savitzky-Golay method with a "window size" 3.

2.5. ESI-MS

Mass spectra were acquired on a LXQ-linear ion trap (THERMO Scientific, San Jose, USA) instrument equipped with an electrospray source. Electrospray full scan spectra in the range of m/z = 50–2000 amu were obtained by infusion through a fused silica tubing at 2–10 µL/min. The samples were analyzed in the negative mode. The LXQ calibration (m/z = 50–2000) was achieved according to the standard calibration procedure from the manufacturer (using a mixture of caffeine, MRFA and Ultramark 1621). The temperature of the heated capillary for the LXQ was set in a range of 200–250 °C, the ion-spray voltage was adjusted to 3–6 kV and the injection time varied between 5–200 ms. The ligand concentration was $c \sim 100$ µM in ammonium acetate buffer (pH = 6.9, c_{buffer} = 20 mM) / acetonitrile, 90/10, V/V. Three samples were prepared for each peptide with 0.9 and 2.0 equivalents of copper(I).

2.6. Determination of apparent stability constants

The affinity constants for the Cu(I)-binding of the different peptides were determined by competition reactions using BCA as a competitor [33]. Three samples were prepared from each peptide ($c_{peptide} \sim 65$ µM, in phosphate buffer, pH = 7.4, c_{buffer} = 20 mM) containing 0.9 equivalents of Cu(I) relative to the concentration of the peptides. As the next step, different equivalents of the competitor, relative to the Cu(I)-content, were added. The progression of the displacement of Cu(I) from the peptide complexes was followed by the measurement of the absorbance of the $[Cu(BCA)_2]^{3-}$ complex (λ_{max} = 562 nm; ε = 7900 M^{-1} cm^{-1}; $\log\beta_2$ = 17.2 [33]). The samples were equilibrated for several days in order to ensure that the recorded spectra represented the state of equilibrium.

3. Results and discussion

3.1. The mononuclear Cu(I) complexes evidenced by UV/Vis and CD spectroscopies

UV/Vis spectroscopic measurements were performed by adding aliquots of a Cu(I) stock solution in acetonitrile to the samples of peptides in phosphate buffer at pH 7.4. The observed changes for the Cu(I)-**VC** system are presented in Fig. 1, while the UV/Vis spectra obtained for Cu(I)-**EC** and Cu(I)-**HS** are shown in the Supplementary data (Fig. S1). The increase of the Cu(I) concentration is accompanied by the appearance of two main absorption bands at $\lambda \sim 260$ nm and $\lambda \sim 300$ nm (Fig. 1 and Fig. S1). The first one refers to a characteristic charge transfer transition from a thiolate group to Cu(I) (LMCT) [34] indicating the coordination of the ligands to Cu(I) via the thiolate moieties of the cysteine residues. The lower energy band appearing around $\lambda \sim 300$ nm was previously attributed to copper-thiolate clusters in metallothioneins [7]. However, such a band was also present in the spectra of other short peptides containing two cysteines where the exclusive formation of mononuclear complexes was proved by diffusion NMR [23]. In excess of Cu(I) a third transition emerges in the UV spectra at $\lambda \sim 340$ nm representing a formally spin-forbidden 3d → 4s metal to metal transition [7,35] indicating the formation of copper-thiolate clusters, as often observed in the interaction of Cu(I) with thiol compounds [6,7,35,36]. The evolution of the LMCT band at 260 nm in all three Cu(I)-peptide systems, relative to the concentration of Cu(I), reflect molar absorbances in the range of ~7000 M^{-1} cm^{-1} per bound Cu(I) ions, which is compatible with values reported for other thiol compounds and for metallothioneins [7,37].

The recorded absorbance at 264 nm increases linearly until a breakpoint at ca.1.4 equivalents of Cu(I) in case of **VC** (Fig. 1) and **HS** (Fig. S1), while in the sample of **EC** (Fig. S1) the increasing absorbance follows a non-linear trend, which might suggest that the complex formation occurs in separated stages. A similar phenomenon was observed by Le Brun and co-workers in the Cu(I)-titration of the copper chaperone CopZ, possessing an MXCXXC metal binding fragment [38]. It was proposed that two major forms of the Cu(I)-CopZ complex existed, depending on the applied Cu(I)-to-protein ra-

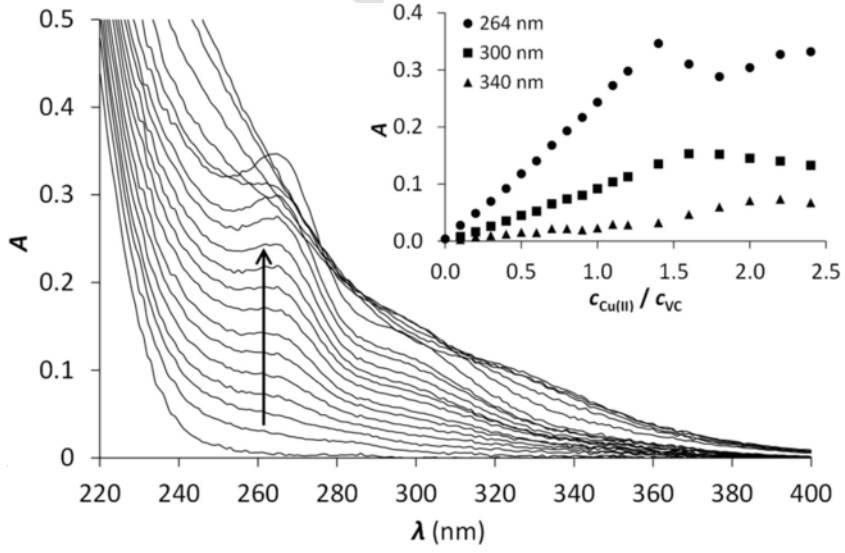

Fig. 1. UV titration of **VC** with Cu(I) at pH = 7.4. The insert shows the absorbances at 264, 300 and 340 nm as a function of the $c_{Cu(I)}/c_{VC}$ ratio. (c_{VC} = 30.0 µM) (*single column*).

tio. Cu(I)$(CopZ)_2$ dominates at low Cu(I)-protein stoichiometries, where only one Cys residue of each monomer is coordinated to the metal ion. The latter species transforms into the dimeric structure $Cu(I)_2(CopZ)_2$ above 0.5:1 Cu(I)-protein ratio, where all the four Cys take part in the coordination, two of them bridging the two Cu(I) ions. The formation of these two Cu(I)-CopZ complexes was more evident on the CD titrations, which showed two clear endpoints at 0.5 and 1 Cu(I) equivalents on the evolution of LMCT bands.

CD spectroscopy is also a useful tool for studying metal ion complexes of peptides since it provides information about the chiral backbone and also about the charge transfer transitions. Thus we attempted to obtain complementary information on the Cu(I)-coordination by **EC**, **VC** and **HS**. The intense negative CD band below 220 nm is attributed to $\pi \rightarrow \pi*$ transitions possibly overlapping with $n \rightarrow \pi*$ transitions, both belonging to the amide bonds of the peptide backbone [39,40] with an essentially disordered structure [25,26,41]. The addition of aliquots of a Cu(I) solution to the ligands results in a gradual change of the intensities at $\lambda = 220$ nm, referring to changes in the average conformation of the ligands induced by metal ion ligation (Fig. 2 and Fig. S2). However, similarly to the UV–Vis, the main information in the CD spectroscopy can be obtained from the $S^- \rightarrow Cu(I)$ LMCT bands. When the peptides were titrated by Cu(I), CD-bands appeared in the 240–380 nm wavelength range in parallel with the increasing Cu(I) concentration. With all the three peptides, up to 1.0 equivalent of Cu(I), the ellipticity at ca. 260 nm follows a linearly increasing trend in parallel with the increasing Cu(I):peptide concentration ratio (see the inserts of Fig. 2 and Fig. S2) and isodichroic points are systematically observed. These results unambiguously show that the free **VC**, **EC** and **HS** peptides are transformed into one single complex species up to reaching the 1:1 Cu(I):peptide ratio. Only the CuL mononuclear complexes are formed with all the peptides, even with **EC**, where presence of more than one species was suspected based on the UV-data.

A further proof that the Cu(I)**EC** complex is the only formed species for Cu(I):**EC** ratios below 1 and that a CuS_4 type Cu(**EC**)$_2$ complex does not exist was obtained by using mercury(II) as a metal ion competitor. A sample with a Cu(I):**EC** ratio of 0.5:1 was titrated with Hg(II). The S^--Cu(I) LMCT (~264 nm) does not change significantly until 0.5 equivalents of Hg(II) as can be seen in Fig. 3. This suggests that the highly thiophilic Hg(II) can find free thiolates to coordinate to and does not disturb the Cu(I) coordination center. The slight increase can be attributed to the overlapping effect of the $S^- \rightarrow Hg(II)$ LMCT below $\lambda = 220$ nm [23,26,42–45]. For further addition of Hg(II) the S^--Cu(I) LMCT starts to collapse, while the S^--Hg(II) LMCT continues to increase, evidencing the transformation of Cu(**EC**) into the more stable Hg(**EC**) complex. These observations confirm that the CuS_4 type Cu(**EC**)$_2$ complex does not exist.

Comparison of the CD spectra obtained at 1:1 $c_{Cu(I)}$:$c_{peptide}$ ratios for the three ligands reflect a notable difference between **HS** and the other two peptides (Fig. 2, Fig. S2, see spectra denoted by letter "b"). Considering that the CD-features observed for the free peptides are rather similar to each other, the different shapes of the CD spectra of the Cu(I) complexes must be correlated to different structures around the Cu(I) ion. Indeed, the absence of prolines in **HS** provides a larger conformational flexibility of the peptide backbone, which may adopt different conformations compared to **VC** and **EC**, affecting the Cu(I) center. Nevertheless, the most plausible explanation for the different CD-features of Cu(I)-**HS** may be the participation of the histidine residue in Cu(I) coordination, as it was demonstrated before for a few Cu(I)-binding proteins and model peptides [46–48]. An additional coordinating donor group besides the two thiolates should modify the chiral environment of the metal ion and therefore change the shape of CD-spectra.

3.2. Polynuclear Cu(I) complexes in excess of metal ions evidenced by UV/Vis and CD spectroscopies

The speciation in any of the Cu(I)-peptide systems above one equivalent of Cu(I) per ligand is rather complex, as reflected by the changes in the UV/Vis. The formation of clusters is indicated by the emerging UV-band at $\lambda \sim 340$ nm. Pronounced changes are also observed in the shapes of the CD spectra, when Cu(I) is added in excess to any of the ligands, which indicates a rather complex speciation, as a possible result of the formation of different clusters or polymetallic structures.

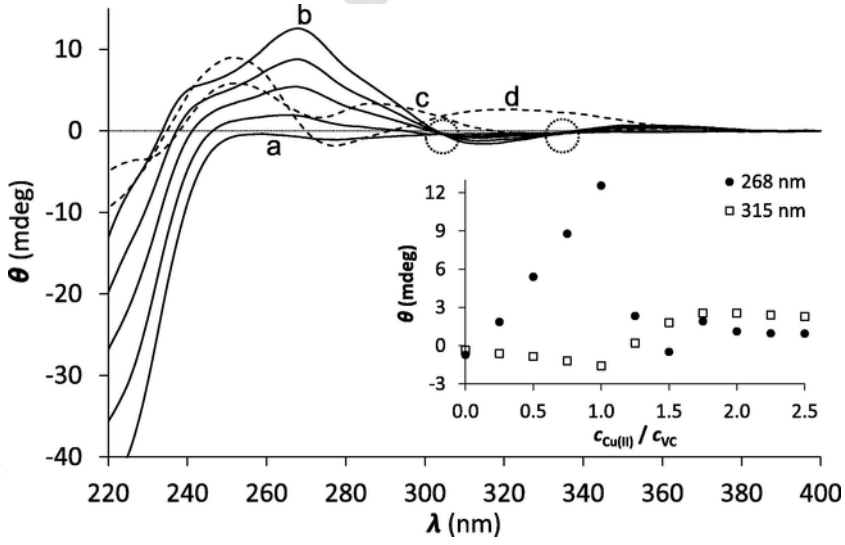

Fig. 2. CD spectra of the **VC** peptide titrated with Cu(I) at pH = 7.4 from 0.0 to 1.0 equivalents of Cu(I) (solid lines). Spectra denoted by the letters "a", "b", "c" and "d" represent samples of 0.0, 1.0, 1.25 and 2.0 equivalents of Cu(I), respectively. Dotted circles highlight isodichroic points. The insert shows the evolution of ellipticities at two selected wavelength values. (c_{VC} = 80 μM) (*single column*).

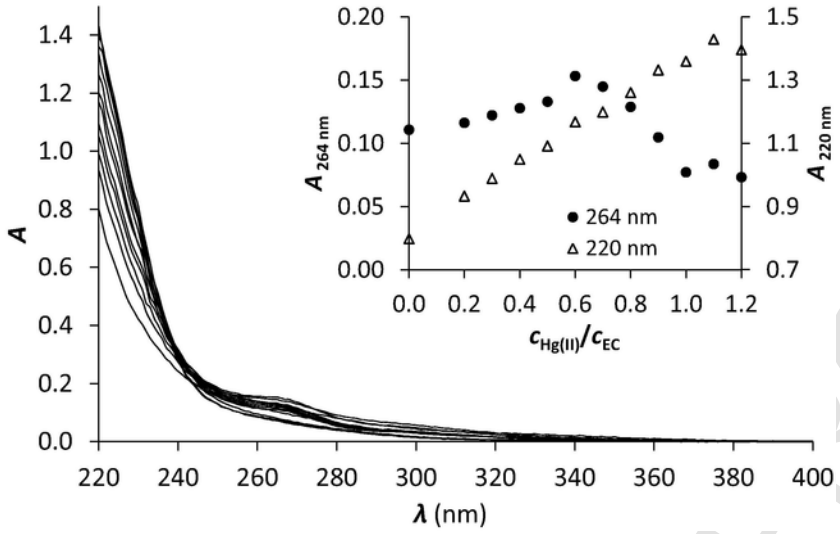

Fig. 3. UV spectra for Cu(I):**EC** 0.5:1 titrated with Hg(II) at pH = 7.4. The insert shows the absorbances at 264 nm (left axis) and 220 nm (right axis) as a function of the $c_{Hg(II)}/c_{EC}$ ratio. (*single column*).

The recorded absorbance values at 260 and 300 nm continue to follow a close to linear increasing trend even up to ~1.3–1.5 equivalents of Cu(I) per peptide (Fig. 1 and Fig. S1), even though CD titrations show clear endpoints at 1 Cu(I) equivalent. This shows that the LMCT absorbance band at ca. 260 nm is not sensitive to the nature of the different complexes (monometallic or polymetallic) but only to the number of thiolate to Cu(I) bonds. A similar behaviour was observed previously for tripodal pseudopeptide ligands bearing three cysteines or D-penicillamines [37,49,50], where the LMCT at 260 nm increased linearly up to 2.0 equiv. of Cu(I), even though it was demonstrated that two different types of complexes formed, the mononuclear CuL from 0.0 to 1.0 equivalent Cu(I) and the Cu_4L_2 or Cu_6L_3 clusters in excess of Cu(I). This indicates that the average number of thiolate-Cu(I) bonds per metal ion does not change significantly in the species formed at low Cu(I) excess over the ligands and accordingly the molar absorbance per bound Cu(I) ion may also be similar to that of the monomeric complex. The nature and formation of these polymetallic species could be inferred by ESI-MS that is sensitive to the stoichiometry of the complexes.

3.3. ESI-MS experiments for studying the nuclearity of the complexes

Samples containing the peptides and 0.9 and 2 equivalents of Cu(I) in ammonium acetate buffer were analyzed by (−)ESI-MS. 10% acetonitrile in volume was added to minimize Cu(I) oxidation during the injection. The spectra acquired for the **EC** peptide are shown in Fig. 4 as an example. For 0.9 equivalent of Cu(I), the major signals arise from the free ligand as the negatively charged ions $[L\text{-}H]^-$ and $[L{-}2H]^{2-}$: m/z = 1202.3 and 600.8, respectively (Fig. 4 upper panel). The CuL complex is detected as a significant species as $[L{+}Cu{-}2H]^-$ and $[L{+}Cu{-}3H]^{2-}$: m/z = 1264.2 and 631.7, respectively (Fig. 4 upper panel). Similar observations can be seen in Fig. S3 for peptides **VC** and **HS**.

Many different polymetallic species were detected with 2 Cu(I) equivalents per ligands (see Fig. 4 lower panel for **EC** as an example): Cu_2(**EC**), Cu_3(**EC**), Cu_4(**EC**)$_2$. Similar mixtures of polymetallic complexes are detected for the three peptides as seen in Fig. S3 for **VC** and **HS**. The isotopic patterns of the Cu(I) complexes formed with the three peptides are shown in Fig. S4.

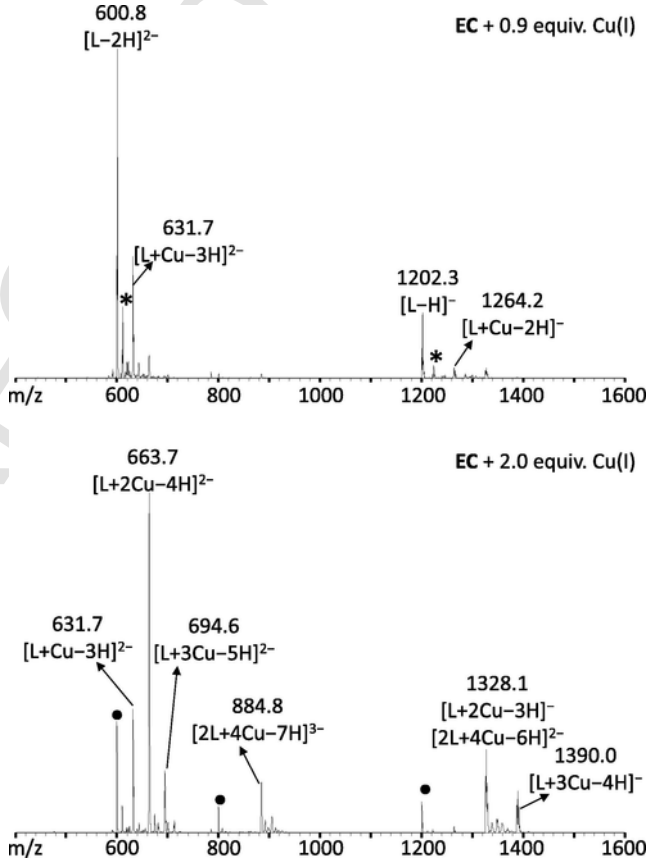

Fig. 4. (−)ESI-MS spectra recorded for Cu(I)-E**C** 0.9:1 (upper panel) and 2:1 (lower panel) systems. * sodium adduct of the free peptide, ● oxidized free peptide (*single column*).

The qualitative results obtained by ESI-MS provide a further support for the Cu(I):L ratio dependent speciation suggested in each of the studied systems based on the UV/Vis and CD-data. They also confirm the complicated speciation in excess of Cu(I).

3.4. Effect of pH on thiolate-binding to Cu(I)

The evolution of the LMCT bands in the Cu(I)L complexes was studied with pH as seen in Fig. 5 reporting the absorbance at 264 nm as a function of pH. The absorbance recorded in the three systems is stable at pH larger than 7 showing that the complexes are fully formed, with absorption coefficients in the range 6300–7800 M^{-1} cm^{-1}. When the pH decreases, two successive processes are detected for each Cu(I) complex. The data were satisfactorily fitted with SPECFIT [51–54], with two successive (de)protonation steps according to equilibrium (1) and (2); the corresponding apparent pK_a values are given in Table 1.

$$CuL + H \rightleftharpoons CuLH \qquad K_1^H = (K_{a1})^{-1} \tag{1}$$

$$CuLH + H \rightleftharpoons CuLH_2 \qquad K_2^H = (K_{a2})^{-1} \tag{2}$$

The first protonation takes place with $\log K^H_1$ values between 3.6 and 5.5 and corresponds to the loss of about half the intensity of the S^- to Cu(I) LMCT absorbance of the Cu(I) complex at pH 7. This is consistent with the protonation of one of the cysteines in equilibrium (1) to give a Cu(I) complex with only one thiolate coordinated to the metal center. The apparent $\log K^H_1$ values found for the three complexes are significantly lower than the $\log K^H$ (=pK_a) previously reported for the Ag(I) complexes formed with **EC** and **VC** (pK_a = 6.5) [27]. The protonation processes reported here for the three Cu(I) peptide complexes are irrelevant with regard to the ways of potential Cu(I)-sequestration in physiological conditions since they are all taking place at pH values significantly lower than pH 7.4. The second protonation steps are detected for lower pH values, with apparent $\log K^H_2$ between 1.3 and 3.0, and result in a total loss of the LMCT absorption to form the $CuLH_2$ complexes with no thiolate bound to Cu(I), according to equilibrium (2). The latter species in acidic conditions may be low stability Cu(I) complexes in which the metal center is coordinated to other functions than thiolates, or may represent the total release of free Cu(I) from the protonated ligand.

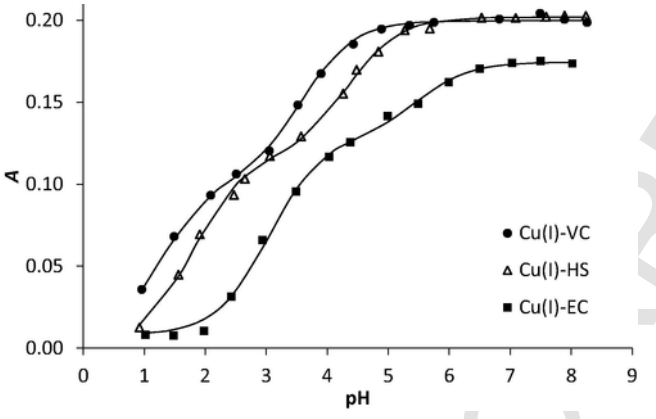

Fig. 5. Absorbances recorded at λ = 264 nm in the Cu(I):peptide 0.9:1 systems as a function of pH. The continuous lines represent the fitted values for the same wavelength. Data fitting was performed by SPECFIT in the wavelength range of λ = 250–400 nm based on a simple model involving two Cu(I)-promoted thiol deprotonation processes (see details in the text) (*single column*).

Table 1
Apparent stability constants of the Cu(I)-peptide complexes at pH = 7.4, apparent pK_a (= $\log K^H$) values and absorption coefficients of the Cu(I)-peptide complexes. Experimental errors on the last characters are indicated in parentheses.

Ligand	$\log \beta_{11}^{pH7.4}$	pK_{a1}	pK_{a2}	ε (M^{-1} cm^{-1}) (264 nm)
EC	15.3(1)	5.5(3)	3.0(1)	6370
VC	15.8(1)	3.6(2)	1.3(2)	7825
HS	16.3(1)	4.3(2)	1.8(1)	7740

3.5. Stability of the Cu(I)-peptide complexes at pH 7.4

The various spectroscopic studies used for the characterization of the Cu(I)-binding of **VC**, **HS** and **EC** demonstrate that mononuclear complexes dominate in solutions where the Cu(I):peptide ratio is close to 1:1. The apparent stability constant of these species at pH = 7.4 were determined by a competition reaction. Previous studies showed that the Cu(I)-binding affinity of two cysteine containing linear or cyclic peptides should fall in the range of $\log\beta_{11}^{pH\ 7.4} \sim 15–17$, $\beta_{11}^{pH\ 7.4}$ being the conditional stability constant of the Cu(I) complex at pH 7.4 [23,24]. According to Wedd's recommendation [33,55] bathocuproine disulfonate (BCS) is a perfect choice for a competitor ligand to conveniently determine stabilities with a $\log\beta_{11}^{pH\ 7.4}$ value near 17 ($\log\beta_2$ ($[Cu(BCS)_2]^{3-}$) = 19.8 [32]). Nevertheless, BCS proved to be a too strong competitor for the three studied systems and only 2 equivalents of the compound relative to Cu(I) withdrew more than 50% of Cu(I) from its peptide complexes. Accordingly, the weaker competitor bicinchoninate anion (BCA) was applied for the determination of the Cu(I)-peptide affinities. BCA forms a well-defined 1:2 complex with Cu(I) according to Eq. (3) characterized by $\log\beta_2$ = 17.2

$$Cu^+ + 2BCA^{2-} \rightleftharpoons [Cu(BCA)_2]^{3-} \tag{3}$$

Addition of BCA to the Cu(I)-peptide solutions results in the appearance of the intense absorption band of the $[Cu(BCA)_2]^{3-}$ complex (λ_{max} = 562 nm, ε = 7900 M^{-1} cm^{-1} [33]), corresponding to the transfer of the metal ion from the peptide to BCA. In order to minimize the risk of the formation of oligometallic species the competition experiments were performed with peptide solutions containing 0.9 equivalent of Cu(I) per peptides. The first indication for the magnitude of the Cu(I)-binding affinity of the peptides is the number of BCA equivalents required for withdrawing 50% of Cu(I) from its peptide complexes. To achieve this, 8, 16 and 24 equivalents of BCA is needed for the samples of Cu(I)-**EC**, Cu(I)-**VC** and Cu(I)-**HS**, respectively, indicating the weakest Cu(I)-binding with **EC** and the strongest with **HS**. The calculated conditional stability constants, summarised in Table 1, match rather well to the affinities obtained for linear and cyclic peptidic models of the Atx1 Cu-chaperone [23,24], in spite of the larger distance between the two cysteine residues in the presently studied dodecapeptides. The lowest affinity of **EC** may be explained by charge repulsion between the three aspartate residues, as found also with other Cu(I) chelating ligands possessing several negatively charged residues near the Cu(I)-binding site [24,37]. The stronger Cu(I)-binding affinity of **HS** can be the result of the higher flexibility of the peptide backbone, which helps the peptide to more easily adopt the optimal coordination geometry. As hinted above on the basis of the CD-results, the histidine residue may directly participate in the coordination of Cu(I) and thus contribute to the higher affinity of **HS** to Cu(I). The stability constants determined in this study (Table 1) are very close to the affinity constant estimated for

the Ag(I)-binding of **VC** ($\log\beta_{11}^{pH8.0} \sim 15–16$), also by a competition experiment [56]. Similarly to what was concluded for Ag(I), being another cognate metal ion of CueR, the Cu(I)-binding affinities of these peptidic models are 5–6 orders of magnitude lower, than that of the native protein [21] which is a possible consequence of a loss of entropy upon metal ion binding of the models [27] but also the lack of other potential stabilizing effects, e.g. hydrophobic interactions in the metal binding pocket or the overall charge neutralisation that operate in the protein in contrast to the models.

4. Conclusion

The three studied oligopeptides (**EC**, **VC** and **HS**), inspired by the metal binding loop of the bacterial copper efflux regulator CueR protein, display similar Cu(I)-binding features in terms of the key role of the two Cys-thiolates in determining the speciation and the stability of complexes formed under neutral conditions but also some notable differences originating from the different amino acid sequences. Monomeric (CuL) complexes dominate at pH = 7.4 and in the presence of ligand excess (even up to a 1:1 Cu(I):L ratio), i.e. under conditions that are relevant for the Cu(I)-binding/transferring actions of proteins participating in Cu-homeostasis. Cu(I)-excess results in a complicated speciation with the formation of thiolate-bound oligometallic/cluster species of various composition. pH titrations showed that deprotonation and coordination of the second thiol group in the Cu-peptide monomeric complexes takes place significantly below neutral pH. This is a remarkable difference compared to what was reported for the Ag(I)-binding of **EC** and **VC** [27]. Consequently, such a (de)protonation process cannot play a role in Cu(I)-sequestration by these peptides in physiological conditions. The Cu(I)-binding affinities of the ligands reflect relatively small but still significant differences likely to be attributed to the destabilizing effect of charge repulsion between the carboxylate sidechain groups in **EC** and the stabilizing effect of the possible direct metal ion coordination of His together with a larger ligand flexibility in **HS**. The magnitude of the conditional stability constants determined at pH = 7.4 ($\log\beta_{11}^{pH\ 7.4} = 15.3–16.3$) fall in the range usually found for other peptide sequences containing two cysteines, being somewhat smaller than those obtained for models of the Atx1 copper chaperone ($\log\beta_{11}^{pH\ 7.4} = 17.4$) [23,24] and comparing well with more rigid cyclic decapeptides encompassing CxxxxC sequences ($\log\beta_{11}^{pH\ 7.4} = 15.5–16.7$) [23,24]. Our results compared to previous ones also demonstrate that the affinity of peptide sequences with two cysteines for Cu(I) depends little on the flexibility of the loop and the number (x) of amino acids in between the two Cys residues (x = 2–7). Therefore, the driving force for the coordination of the soft Cu(I) cation is expected to be mainly the formation of the two strong bonds with the soft thiolate donors.

The oligopeptide models described in this paper do not reproduce the zeptomolar (10^{-21} M) sensitivity of the regulator protein CueR or its specificity for monovalent versus divalent cations [21], exemplifying the complexity of metal regulation processes *in vivo*, which cannot simply be described by thermodynamic equilibria. However, the studied model peptides still resemble the ability of the protein to exclusively accommodate one metal ion per sequence under ligand excess conditions. Finally, these model peptides show large affinities for Cu(I) combined with high selectivities vs. Zn(II) [26], which are features that may be utilized in the development of Cu(I)-sequestering agents [28].

Acknowledgements

This research was supported by the Labex ARCANE (Grant ANR-11-LABX-0003-01), the "Fondation pour la Recherche Médicale" (grant DCM20111223043), the Hungarian National Research, Development and Innovation Office-NKFIH through project GINOP-2.3.2-15-2016-00038 and grant No: K_16/120130.

References

[1] R.A. Festa, D.J. Thiele, Curr. Biol. 21 (2011) R877–R883.
[2] R.G. Pearson, J. Am. Chem. Soc. 85 (1963) 3533–3539.
[3] R.R. Conry, Encyclopedia of Inorganic Chemistry, John Wiley & Sons Ltd, 2006.
[4] K.A. Koch, M.M.O. Peña, D.J. Thiele, Chem. Biol. 4 (1997) 549–560.
[5] R.D. Palmiter, Proc. Natl. Acad. Sci. U.S.A. 95 (1998) 8428–8430.
[6] P. Faller, M. Vašák, Biochemistry 36 (1997) 13341–13348.
[7] D.L. Pountney, I. Schauwecker, J. Zarn, M. Vasak, Biochemistry 33 (1994) 9699–9705.
[8] A. Dancis, D.S. Yuan, D. Haile, C. Askwith, D. Eide, C. Moehle, J. Kaplan, R.D. Klausner, Cell 76 (1994) 393–402.
[9] K. Petrukhin, S. Lutsenko, M.J. Cooper, C.T. Gilliam, J.H. Kaplan, J. Biol. Chem. 272 (1997) 18939–18944.
[10] P.A. Cobine, G.N. George, C.E. Jones, W.A. Wickramasinghe, M. Solioz, C.T. Dameron, Biochemistry 41 (2002) 5822–5829.
[11] F. Arnesano, L. Banci, I. Bertini, S. Mangani, A.R. Thompsett, Proc. Natl. Acad. Sci. U.S.A. 100 (2003) 3814–3819.
[12] I.R. Loftin, S. Franke, N.J. Blackburn, M.M. McEvoy, Prot. Sci. 16 (2007) 2287–2293.
[13] Y. Xue, A.V. Davis, G. Balakrishnan, J.P. Stasser, B.M. Staehlin, P. Focia, T.G. Spiro, J.E. Penner-Hahn, T.V. O'Halloran, Nat. Chem. Biol. 4 (2008) 107–109.
[14] A.C. Rosenzweig, Chem. Biol. 9 (2002) 673–677.
[15] F.W. Outten, C.E. Outten, J. Hale, T.V. O'Halloran, J. Biol. Chem. 275 (2000). 31024-31029.
[16] J.V. Stoyanov, J.L. Hobman, N.L. Brown, Mol. Microbiol. 39 (2001) 502–512.
[17] N.L. Brown, J.V. Stoyanov, S.P. Kidd, J.L. Hobman, F.E.M.S. Microbiol, Rev. 27 (2003) 145–163.
[18] C. Rensing, B. Fan, R. Sharma, B. Mitra, B.P. Rosen, Proc. Natl. Acad. Sci. U.S.A. 97 (2000) 652–656.
[19] G. Grass, C. Rensing, Biochem. Biophys. Res. Commun. 286 (2001) 902–908.
[20] C. Rademacher, B. Masepohl, Microbiology 158 (2012) 2451–2464.
[21] A. Changela, K. Chen, Y. Xue, J. Holschen, C.E. Outten, T.V. Halloran, A. Mondragón, Science 301 (2003) 1383–1387.
[22] O. Seneque, S. Crouzy, D. Boturyn, P. Dumy, M. Ferrand, P. Delangle, Chem. Commun. (2004) 770–771.
[23] P. Rousselot-Pailley, O. Sénèque, C. Lebrun, S. Crouzy, D. Boturyn, P. Dumy, M. Ferrand, P. Delangle, Inorg. Chem. 45 (2006) 5510–5520.
[24] A.M. Pujol, M. Cuillel, O. Renaudet, C. Lebrun, P. Charbonnier, D. Cassio, C. Gateau, P. Dumy, E. Mintz, P. Delangle, J. Am. Chem. Soc. 133 (2011) 286–296.
[25] A. Jancso, D. Szunyogh, F.H. Larsen, P.W. Thulstrup, N.J. Christensen, B. Gyurcsik, L. Hemmingsen, Metallomics 3 (2011) 1331–1339.
[26] D. Szunyogh, B. Gyurcsik, F.H. Larsen, M. Stachura, P.W. Thulstrup, L. Hemmingsen, A. Jancso, Dalton Trans. 44 (2015) 12576–12588.
[27] D. Szunyogh, H. Szokolai, P.W. Thulstrup, F.H. Larsen, B. Gyurcsik, N.J. Christensen, M. Stachura, L. Hemmingsen, A. Jancsó, Angew. Chem. Int. Ed. 54 (2015) 15756–15761.
[28] P. Delangle, E. Mintz, Dalton Trans. 41 (2012) 6359–6370.
[29] P. Kamau, R.B. Jordan, Inorg. Chem. 40 (2001) 3879–3883.
[30] P.W. Riddles, R.L. Blakeley, B. Zerner, Methods in Enzymology, Academic Press, 198349–60.
[31] G.L. Ellman, Arch. Biochem. Biophys. 82 (1959) 70–77.
[32] Z. Xiao, F. Loughlin, G.N. George, G.J. Howlett, A.G. Wedd, J. Am. Chem. Soc. 126 (2004) 3081–3090.
[33] Z. Xiao, L. Gottschlich, R. van der Meulen, S.R. Udagedara, A.G. Wedd, Metallomics 5 (2013) 501–513.
[34] M. Beltramini, K. Lerch, Biochemistry 22 (1983) 2043–2048.
[35] R. Bogumil, P. Faller, D.L. Pountney, M. Vašák, Eur. J. Biochem. 238 (1996) 698–705.
[36] K. Fujisawa, S. Imai, N. Kitajima, Y. Moro-oka, Inorg. Chem. 37 (1998) 168–169.
[37] A.M. Pujol, C. Gateau, C. Lebrun, P. Delangle, Chem. Eur. J. 17 (2011) 4418–4428.
[38] M.A. Kihlken, A.P. Leech, N.E. Le Brun, Biochem. J. 368 (2002) 729.

[39] Y.J. Li, U. Weser, Inorg. Chem. 31 (1992) 5526–5533.
[40] S.M. Kelly, N.C. Price, Curr. Protein Pept. Sci. 1 (2000) 349–384.
[41] A. Jancsó, B. Gyurcsik, E. Mesterházy, R. Berkecz, J. Inorg. Biochem. 126 (2013) 96–103.
[42] G.R. Dieckmann, D.K. McRorie, D.L. Tierney, L.M. Utschig, C.P. Singer, T.V. O'Halloran, J.E. Penner-Hahn, W.F. DeGrado, V.L. Pecoraro, J. Am. Chem. Soc. 119 (1997) 6195–6196.
[43] A.M. Pujol, C. Lebrun, C. Gateau, A. Manceau, P. Delangle, Eur. J. Inorg. Chem. 2012 (2012) 3835–3843.
[44] S. Pires, J. Habjanič, M. Sezer, C.M. Soares, L. Hemmingsen, O. Iranzo, Inorg. Chem. 51 (2012) 11339–11348.
[45] M. Łuczkowski, B.A. Zeider, A.V.H. Hinz, M. Stachura, S. Chakraborty, L. Hemmingsen, D.L. Huffman, V.L. Pecoraro, Chem. Eur. J. 19 (2013) 9042–9049.
[46] L. Zhang, M. Koay, M.J. Maher, Z. Xiao, A.G. Wedd, J. Am. Chem. Soc. 128 (2006) 5834–5850.
[47] M.J. Pushie, K. Shaw, K.J. Franz, J. Shearer, K.L. Haas, Inorg. Chem. 54 (2015) 8544–8551.
[48] K.L. Haas, A.B. Putterman, D.R. White, D.J. Thiele, K.J. Franz, J. Am. Chem. Soc. 133 (2011) 4427–4437.
[49] A.-S. Jullien, C. Gateau, C. Lebrun, I. Kieffer, D. Testemale, P. Delangle, Inorg. Chem. 53 (2014) 5229–5239.
[50] A.M. Pujol, C. Gateau, C. Lebrun, P. Delangle, J. Am. Chem. Soc. 131 (2009) 6928–6929.
[51] H. Gampp, M. Maeder, C.J. Meyer, A.D. Zuberbühler, Talanta 32 (1985) 1133–1139.
[52] H. Gampp, M. Maeder, C.J. Meyer, A.D. Zuberbühler, Talanta 32 (1985) 257–264.
[53] H. Gampp, M. Maeder, C.J. Meyer, A.D. Zuberbühler, Talanta 32 (1985) 95–101.
[54] H. Gampp, M. Maeder, C.J. Meyer, A.D. Zuberbühler, Talanta 33 (1986) 943–951.
[55] Z. Xiao, A.G. Wedd, Nat. Prod. Rep. 27 (2010) 768–789.
[56] A. Jancso, unpublished results, 2015.